A Comprehensive Evaluation on Variable Sampling Intervals of Power Battery System for Electric Vehicles

SHICHUN YANG, (Member, IEEE), YAOGUANG CAO, SIDA ZHOU, YANG HUA, XINAN ZHOU, AND XINHUA LIU

School of Transportation Science and Engineering, Beihang University, Beijing 100191, China

Corresponding author: Xinhua Liu (liuxinhua19@buaa.edu.cn)

ABSTRACT Considered to be the state-of-art solution for intelligent management of electric vehicles, cloud-control has been broadly investigated especially for parameterization and state estimation. Considering the operational cloud-database, the sampling intervals contribute to the precision and robustness of the battery management, and a balance between storage and performance is of crucial importance for real-time controlling. Unfortunately, the comprehensive performances on variable sampling intervals are doubtful for the development of cloud-control. Herein, the research of sampling intervals is carried out and the operational applications are simulated for validation including the precision, robustness and information content. 5th-order spherical simplex-redial Kalman filter and particle swarm optimization-simulated annealing methods are developed for researching the influences on precision of state of charge (SOC) estimation and parameterization under stable or dynamic conditions. Moreover, the information content of the desecrated database is evaluated based on the information entropy. The comparative results are carried out for separate characteristic, and the analysis exhibit the special performances for diverse sampling interval. The research confirms the differences on diverse intervals on operational applications, and the analysis might deliver effective guidance for future processing framework based on cloud-controlling towards specific intentions.

INDEX TERMS Lithium-ion batteries, battery management systems, sampling intervals, state-of-charge, parameterization, remote control, complex networks.

I. INTRODUCTION

As world increasingly concerning the pollution and energy crisis, electric vehicles (EVs) have been regarded as one of the feasible solutions for substituting the fuel with electricity. Considered to be preferable components for EVs, the lithium-ion batteries have been developed for operational applications owing to multiple facets such as stationary characteristics and reliant lifespan, and the fast-growing markets for applicational EVs which are closely associated with innovative technologies of battery management system (BMS). Deliberated as the crucial components, the management of batteries draws growing attention for both academia and industry due to the unpredictable safety and anxious driving mileage, and the precise modelling and state-of-charge (SOC) estimation are fundamental issues for improving the

comprehensive performance of batteries [1], including energy management strategy [2], health diagnosis [3], lifespan prediction [4] and other related functions.

Considered as the basis states for management, SOC represents the restful charging/discharging capacity, and the evaluation of driving mileage/ safety is associated with precision of SOC estimation. The classical methodologies for modelling and SOC estimation are dependent on the online intelligent embedded system installed on EVs, where BMS engages the communication, sampling and abundant controlling. Unfortunately, the limited computation restricts the operational application for advanced algorithms, and the precision and robustness of BMS are very hard to be guaranteed. Thus, the state-of-art Cyber Hierarchy And Interactional Network (CHAIN) is proposed as a multi-factor and multi-discipline digital solution framework for full-lifespan management of EV power systems, and the cloud-controlling is considered to be progressive approach for resolving the issue of battery

The associate editor coordinating the review of this manuscript and approving it for publication was Jianquan Lu.

management [5]. As the data of various sampling intervals uploading to the cloud-database, the complex algorithms can be carried out on cloud-platform with sufficient computing capability to achieve ideal comprehensive performances, for exampling the remote fault diagnosis [6].

Diverse methodologies for modelling and SOC estimation have been well developed and they might be operational for cloud-controlling. Li *et al.* [7] proposed an equivalent model with physical basement on the purpose for development of computationally-efficient battery control methods. As for SOC estimation, Yang *et al.* [8] developed special and difference model for contributing to the estimation of SOC and capacity. Family of Kalman filters has been broadly investigated for SOC estimation, and the outstanding performance can be achieved under various categories [9]. Combining the multi-time scale extended Kalman filters, the satisfactory precision can be achieved for battery modules. Yan *et al.* [10] introduced adaptive Lebasque sampling particle filter, while the advanced algorithm might have trouble with online applications. Other methodologies for parameterization and SOC estimation can be summarized as TABLE 1.

TABLE 1. Summarization of current researches.

Item	Author	Year	Methodology	Precision
SOC estimation	Hong Jichao [11]	2020	Recurrent neural network with long short-term memories	Under 1%
SOC estimation	Zhang Wenjie [12]	2018	Adaptive battery state estimator for SOC and modelling	3%
SOC estimation	Yang Fangfang [13]	2016	Unscented Kalman filter	3%
SOC estimation	Li Di [14]	2015	Strong tracking sigma point Kalman filter	0.9%
SOC estimation	Wang Yujie [15]	2015	Particle filter	1%
Battery modelling	Yang Jufei [16]	2019	Charging network-based equivalent circuit model	Under 40 mA
Battery modelling	Pang Hui [17]	2019	Doylee Fullere Newman model	Under 2%
Battery modelling	Wang Qian-Kun [18]	2017	Thermal coupled equivalent circuit model	Under 20mV
Parameterization	Komal Saleem [19]	2020	Online Reduced Complexity technique	Under 1%
Parameterization	Petr Vyroubal [20]	2018	Electrochemical impedance spectroscopy	About 100 mV

Generally, the broad researches are fundamental on experimental results and the constant sampling interval is recognized as 1 s. However, the realistic sampling intervals of cloud-database is usually variable especially for lost messages, and the selection of interval has great influences on designs. Considering the interfering sampling, the desecrate database usually suffers from unpredicted information lost, and then the prevalent methods might fail to achieve effective management. The impacts on battery modelling and SOC estimation is unknown, thus the investigation of sampling intervals is necessary. Herein, the analysis for comprehensive influences of variable sampling intervals is carried out, and results confirm the potential guidance for future design of cloud-database. Diverse characterizes are discussed based on rigorous mathematical analysis and the performances on virous sampling intervals for battery are presented. Considering operational applications of the future cloud-controlling platform, specific strategies on the design of platform can be explored based on further investigations.

The second-order equivalent model (SECM) is recognized as modelling implementation of battery on $LiNi_8Co_1Mn_1O_2$ (NCM 811) cathode, and 5th-order simple spherical simplex-radial cubature Kalman filter (SSRCKF) is developed for SOC estimation. Diverse categories of experimental conditions with various sampling intervals are exploited to verify the precision and robustness including stable and dynamic tests. Additionally, the content of information for desecrated database is discussed based on average deviation of the data, and information entropy (IE) theory is adopted to evaluate amount of information, delivering the description of information contents.

II. IMPLEMENTATIONS
A. SECOND-ORDER EQUIVALENT CIRCUIT MODEL
Considering the battery modelling, various categories can be achieved to simulate the dynamic characteristics including electrochemical models [21], equivalent circuit models and data-driven models [22], while the computational effectiveness for further promotion is still of essential for cloud-control. Equivalent circuit models (ECMs) are one of the widely prevalent models applied in embedded BMS, and the effectiveness for online estimation delivers the promotion on future cloud-controlling. The nth-order networks model is the typically simplified one with satisfactory performance. The parallel RC networks describe the dynamic characteristics of the batteries, which represent the polarization reaction internal the batteries. It is proved that the performance of ECMs is associated with battery category, where second-order RC model with one-state hysteresis demonstrates superior availability and performance of $LiFePO_4$ (LFP) cells, while SECM is preferred for $LiNi_xCo_yMn_zO_2$ (NCM) cells [23]. In this article, the SECM model is adopted and a matched battery with NCM 811 cathode.is experimented. The schematic diagram is presented in Figure 1 (a), and the parameter set consists of R_o, R_e, R_c, C_e, C_c. Generally, R_o denotes the internal ohmic resistance and the direct voltage drop caused by current can be simulated on this resistance. The other RC networks indicate the electrochemical polarization reaction and concentration polarization reaction, and two networks are determined with different time constants. The open-circuit-voltage (OCV) is recognized with SOC, and I_L is the current. The mathematical description of SECM is constructed from Kirchhoff's law, and it can be presented as
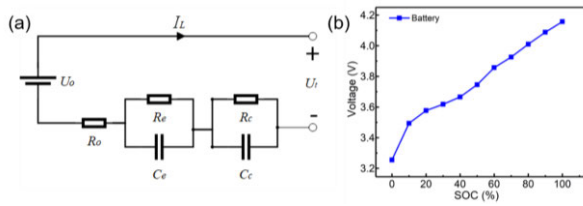
FIGURE 1. The schematic diagram of second-order equivalent model. (a) and open-circuit-voltage curve (b).

equation (1)

$$\begin{cases} U_o = I_L R_o \\ \dot{U}_e = \dfrac{I_L}{C_e} - \dfrac{U_e}{R_e C_e} \\ \dot{U}_c = \dfrac{I_L}{C_c} - \dfrac{U_c}{R_c C_c} \\ U_t = U_{ocv} - U_e - U_c - U_o \end{cases} \quad (1)$$

where: I_L is the sample current; R_o is internal ohmic resistance and U_o is ohmic voltage drop; R_e and C_e indicate the electrochemical polarization reaction; R_c and C_c indicate concentration polarization reaction; U_e, U_c are polarization voltage drop; U_t is the terminal voltage; U_{ocv} is open-circuit-voltage.

The OCV curve can be obtained based on the results of pulse discharging experiment as Figure 1 (b). Additionally, SOC is generally defined as equation (2), and coupling the equation (1) and (2) results in the construction of battery model. Considering the operational application in state-space, the battery model can be desecrated as equation (3). It is worthy to mention that the constructed system model is associated with sampling intervals, and the performance will be influenced as the increasing of intervals. Additionally, only 6 parameters are needed to be identified, and the limited complexity of model leads to the widely promotion on EVs.

$$SOC(t+1) = SOC(t) - \frac{\eta}{Q_C} \int_t^{t+1} I_t dt \quad (2)$$

$$\begin{bmatrix} SOC_{k+1} \\ U_{p1,k+1} \\ U_{p2,k+1} \end{bmatrix} = \begin{bmatrix} 1 & 0 & 0 \\ 0 & e^{-T_s/R_e C_e} & 0 \\ 0 & 0 & e^{-T_s/R_c C_c} \end{bmatrix} \begin{bmatrix} SOC_k \\ U_{p1,k} \\ U_{p2,k} \end{bmatrix}$$
$$+ \begin{bmatrix} -\dfrac{\eta_c T_s}{Q_c} \\ R_{p1}(1 - e^{-T_s/R_e C_e}) \\ R_{p2}(1 - e^{-T_s/R_c C_c}) \end{bmatrix} * I_k + w \quad (3)$$

where: η_c is the Coulomb efficiency, which is can be considered as 0.99; Qc is the nominal capacity experimented from the capacity test; T_s is the sampling interval, which is set as 1; w is the process noise.

B. PARAMETER IDENTIFICATION
The precision of battery model offers the probability for accurate SOC estimation; therefore, it is necessary to determine the modelling parameters carefully to ensure stable operation on improving performance of battery cloud-controlling. Generally, the issue of model parameter identification can be abstract as optimization problem, and various methods can be applied including least square, simulated annealing (SA), particle swarm optimization (PSO) and so on. Considering that OCV can be extracted from the result of pulse discharging experiments, the parameter set to be identified is composed of 6 parameters. Thus, the remaining set can be presented as equation (4) and the optimum object is demonstrated as equation (5). Premeditating the evaluation of parameterization, the root-mean square error (RMSE) between measured terminal voltage and model-simulated voltage is selected as the fitness function, presented as equation (6):

$$\theta = [R_o, R_{p1}, R_{p2}, C_{p1}, C_{p2}]^T \quad (4)$$

$$\arg \min(\{f(\theta)\}) \quad (5)$$

$$RMSE = \sqrt{\frac{1}{N} \sum_{i=1}^{N} \left(\left| V_i - V(\widehat{\theta}) \right| \right)} \quad (6)$$

Considered as intelligent evolutionary parameterization methodologies, SA and PSO are preferable for identifying the battery model since the ability of wider global search while immunizing to local minimum traps. Unfortunately, the contradiction between precision and computational efficiency still restrict the application of both methods. Thus, the coupling particle swarm optimization-simulated annealing (PSO-SA) method is adopted as the algorithm for parameterization and the coupling method is constructed considering the advantage of PSO algorithm for faster convergence and SA algorithm for global searching ability.

The essential governing equation of the developed method is based on PSO, and the results of PSO contribute to the searching process on SA. Herein, each feasible solution can be abstract as a particle with position x and velocity v, and the updating of the states are presented as equation (7) and (8). The fundamental factors are presented as TABLE 2, and it is worthy to mention that the developed method recognizes the factors as constant, while other adaptive methods might be developed for enhancing the performances [24].

$$v_{k+1} = \omega v_k + c_1 r_1 [p_k - x_k] + c_2 r_2 [g_k - x_k] \quad (7)$$

$$x_{k+1} = x_k + v_k \quad (8)$$

where: ω is the inertia weight; c_1 and c_2 are learning factors; r_1 and r_2 are random numbers between 0 and 1; v is the velocity of particle; x is the current solution; p is the individual-best solution; g is the group-best solution.

Resembling the cooling procedure for molten metals through annealing, SA is originated from industrial method where the atoms has the spontaneous attempt to maintain the least internal energy. However, the outstanding characteristics of annealing is the ability for accepting the worse solution on the process of searching the best one, namely Metropolis

TABLE 2. Parameters of improved PSO-SA algorithm.

Item	Description	Value
ω	Inertia weight.	0.8
c1	Self-learning factor	0.8
c2	Swarm-learning factor	1.2
$\xi 1$	Factor to determine the initial temperature	0.527 [26]
$\xi 2$	Factor to determine the final temperature	200 [26]
η	Factor to determine the cooling rate	0.0108 [26]

principle as equations (9). The process of SA is related with the results of PSO, and the cooling scheme is determined from the fitness function of particle swarm. The essential factors of SA include the initial/final temperature and the cooling rate, and the logarithmic cooling scheme is presented as equation (10) to (11). Associated parameters are presented as TABLE 2, and it is worthy to mention that the adopted cooling scheme is based on the particle swarm of PSO, and the factors are determined after the initialization of PSO. Herein, various methods can be applied for determining the factors of PSO [24], [25], and it is considered to be appropriate that the inertia weight should be in $0 - 1$, and the learning factors can be in 0 -2.

$$p_{ij} = \begin{cases} 1 & f(x_j) < f(x_i) \\ \exp(-\dfrac{f(x_j) - f(x_i)}{T}) & f(x_j) \geq f(x_i) \end{cases} \quad (9)$$

$$T_0 = \xi_1 \frac{\pi_0}{20} \quad (10)$$

$$T_n = \xi_2 \frac{\pi_n}{20} \quad (11)$$

$$T_{j+1} = \frac{T_j}{1 + (T_0 - T_n)/(\eta \cdot T_0 T_n) \cdot T_j} \quad (12)$$

where: i refers to the last iteration and j is the current iteration; p_{ij} is the probability for accepting the current solution; f is the optimizing function; T is the annealing temperature; T_0 is the initial temperature and T_n is the final temperature; χ_1, χ_2 and η are factors; π_0 is the maximum of $\{f(x_i) - f(x_{i-1})\}$, and π_n is the minimum of $\{f(x_i) - f(x_{i-1})\}$.

The general process of PSO-SA can be demonstrated as follows:

Step 1: Initialization

Randomly generate serials particles based on Gaussian theory, and calculate the fitness function of all particles. Then determine the factors of cooling scheme as equation (10) to (11).

Step 2: Updating

Update all particles as equation (7) to (8). Then iterate the updating for L times and accept the solution as equation (9).

Step 3: Annealing

Annealing as equation (12), and calculate the annealing temperature T.

Step 4: Optimization

Repeat step 2 and step 3, until the annealing temperature reach the end or the RMSE is less than 10^{-6}.

C. MATHEMATICAL METHODOLOGIES FOR SOC ESTIMATION

Several estimators have been promoted to SOC estimation, while the family of Kalman filters is the preferable one owing to the computational economy principle. Compared with other categories, cubature Kalman filter generally has a better performance for describing the non-linear integrated equations. Originated from Bayesian filtering theory, the serial states are associated with all historical information and observers, presented as equation (13). To simplify the computation and enhance the efficiency, the assumption that the system possesses Markov characteristic as equation (14) is adopted, and the current state is only related to the former state.

$$x \sim p(x_k | x_1, x_2, \ldots, x_{k-1}, z_1, z_2 \ldots, z_{k-1}) \quad (13)$$

$$x \sim p(x_k | x_{k-1}) \quad (14)$$

where: x is the system state with n dimension, z is the observation, and p is the probability.

Although the simplicity obviously reduces the system complexity, the non-linear equation still has trouble with efficient calculation. Thus, the various principles are developed to precisely estimate the equation while with finite computational cost, and spherical-radial principle is one of the efficient approaches. A series of cubature points with diverse weights can be generated to approximate the optimal state of posterior distribution. Here, an innovative spherical-radial principle, namely 5th-order spherical simplex-radial principle (5th-SSR), is developed to achieve a fourth-order approximation to a nonlinear system. The essential key for employing the 5th-SSRCKF is to determine the cubature points, and the associated cubature points can be presented as equation (15) and (19). Considering the complexity of algorithm, the time complexity is $O(n^2 + 3n + 3)$.

$$a_j = [a_{j,1}, a_{j,2}, \cdots, a_{j,n}]^T, \quad j = 1, 2, \cdots, n+1 \quad (15)$$

$$a_{j,i} = \begin{cases} -\sqrt{\dfrac{n+1}{n(n-i+2)(n-i+1)}}, & i < j \\ \sqrt{\dfrac{(n+1)(n-j+1)}{n(n-i+2)}}, & i < j \\ 0, & i < j \end{cases} \quad (16)$$

$$\{b_j\} = \sqrt{\frac{n}{2(n-1)}}(a_i + a_l) : i < l, \quad l = 1, 2, \cdots, n+1 \quad (17)$$

$$\begin{cases} \xi_1 = \bar{x} \\ \xi_{i+1} = \bar{x} + \sqrt{(n+2)P}a_i \\ \xi_{i+n+2} = \bar{x} - \sqrt{(n+2)P}a_i \\ \xi_{i+2n+3} = \bar{x} + \sqrt{(n+2)P}b_i \\ \xi_{i+\frac{n^2}{2}+\frac{5n}{2}+3} = \bar{x} - \sqrt{(n+2)P}b_i \end{cases} \quad (18)$$

$$\begin{cases} w_1 = \dfrac{2}{n+2} \\ w_i = \dfrac{(7-n)n^2}{2(n+1)^2(n+2)^2} \\ w_{i+n} = \dfrac{2(n-1)^2}{(n+1)^2(n+2)^2} \end{cases} \tag{19}$$

5th-SSRCKF can be developed based on the architecture of Kalman filter and 5th-SSR principle is incorporated to enhance the performance of precision and robustness. The procedure of 5th-SSRCKF can be summarized including initialization, prediction, measurement, correction, and updating, and is shown in TABLE 3. It is worthy to

TABLE 3. The explemtary process of SSRCKF.

Battery model equations:
$$\begin{cases} \boldsymbol{x}_k = f(\boldsymbol{x}_{k-1}, \boldsymbol{w}_k) \\ z_k = h(\boldsymbol{x}_k, v_k) \end{cases}$$

Initializations:
$\boldsymbol{x}_0, \boldsymbol{P}_0, \boldsymbol{Q}, R$, n

Prediction

Sampling the cubature points based on last state as equation () to ():

$\boldsymbol{\xi}_{i,k-1}$,i=1,2,…,2n

Predict the state and covariance:

$$\boldsymbol{\xi}_{i,k-1} = f(\boldsymbol{\xi}_{i,k-1}, \boldsymbol{w}_{k-1}) \quad ,i=1,2,…,2n$$

$$\hat{\boldsymbol{x}}_{k|k-1} = \sum_{i=1}^{L} \omega_i \boldsymbol{\xi}_{i,k-1} \quad ,i=1,2,…,2n$$

$$\boldsymbol{P}_{k|k-1} = \sum_{i=1}^{L} \omega_i (\boldsymbol{\xi}_{i,k-1} - \hat{\boldsymbol{x}}_{k|k-1})(\boldsymbol{\xi}_{i,k-1} - \hat{\boldsymbol{x}}_{k|k-1})^T + \boldsymbol{Q}_{k-1} \quad ,i=1,2,…,2n$$

Correction

Sampling the cubature points based on predictive state as equation () to ():

$\boldsymbol{\xi}_{i,k|k-1}$,i=1,2,…,2n

Update the observation and covariance:

$$z_{i,k|k-1} = h(\boldsymbol{\xi}_{i,k|k-1}, \boldsymbol{v}_{k-1})$$

$$\hat{z}_{k|k-1} = \sum_{i=1}^{L} \omega_i z_{i,k|k-1}$$

$$\varepsilon_k = z_k - \hat{z}_{k|k-1}$$

$$P_{zz} = \sum_{i=1}^{L} \omega_i (z_{i,k|k-1} - \hat{z}_{k|k-1})(z_{i,k|k-1} - \hat{z}_{k|k-1})^T + R_{k-1}$$

$$\boldsymbol{P}_{xz} = \sum_{i=1}^{L} \omega_i (\boldsymbol{\xi}_{i,k|k-1} - \hat{\boldsymbol{x}}_{k|k-1})(z_{i,k|k-1} - \hat{z}_{k|k-1})^T$$

$$\boldsymbol{G}_k = \boldsymbol{P}_{xz} P_{zz}^{-1}$$

Updating

$$\hat{\boldsymbol{x}}_k = \hat{\boldsymbol{x}}_{k|k-1} + \boldsymbol{G}_k (z_k - \hat{z}_{k|k-1})$$

$$\boldsymbol{P}_k = \boldsymbol{P}_{k|k-1} - \boldsymbol{G}_k P_{zz} \boldsymbol{G}_k^T$$

mention that the initialization has great influence on the robustness, and unproper initialization may lead to a higher time for convergence. Another factor $\boldsymbol{G}$, namely Kalman gain, indicates the interferences impacted on the system, and ability for convergence is related the gain

D. PERFORMANCE EVALUATION OF SAMPLING INTERVALS

As the increasing of sampling intervals, the demand of information storage is obvious decreasing while the valid data may be neglected owing to inadequate sampling. Considering the serial samplings shown as Figure 2 (a), massive information is neglected when applying an enlarged interval, and thus the dynamic characteristics might be uncovered between two samples as shown in Figure 2 (b). It is obvious that the voltage curve is rather smooth under large sampling intervals, while the kinetics fragments can be maintained under brief intervals. Thus, the degree of information lost is doubtful for varying the intervals, and diverse methods for evaluating the performance of desecrated database is crucial important. Generally, the content of database consists of the average deviation corresponding to the reference, and the quantity of effective information. In this article, the average deviation estimation is introduced to assess the general error, and information entropy theory is developed to determine the information content of the database.
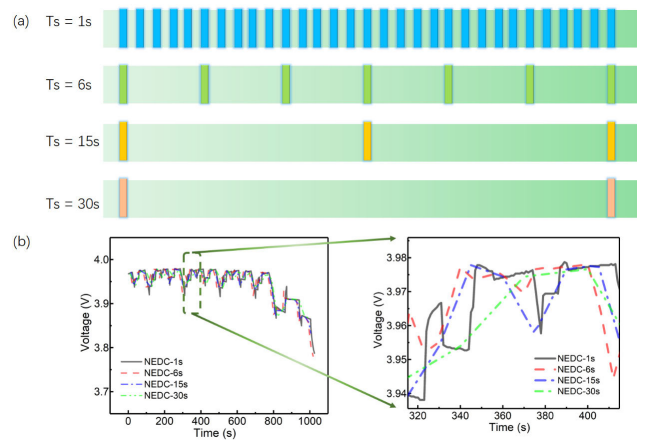
FIGURE 2. The schematic diagram of the discrete database. (a) schematic diagram of the discrete sampling (b) sample of discrete database under different sampling intervals.

1) AVERAGE DEVIATION ESTIMATION

The average deviation E is constructed between the experimental data with simulated result under diverse sampling intervals, and the result demonstrates the general deviation from the database with the average. It is worthy to mention that the sampling interval of reference data is set as 1 s, and other simulated one is recognized as Ts. Considering the difference of sampling between two intervals, the deviation

can be defined as equation (20).

$$E = \sqrt{\frac{1}{N} \sum_{i=1}^{N} \sum_{j=1}^{Ts-1} (x_{reference,j,i} - x_{Ts,i})^2}$$ (20)

where: $x_{\text{reference},i,j}$ is the state under reference sampling interval; $x_{Ts,i}$ is the state under sampling interval of T_s; the subscript j refers to the serial states under reference sampling interval which are between neighboring states under sampling interval of T_s; the subscript i refers to the total count of states under sampling interval of T_s.

The estimation of E can be divided into two parts: one is to estimate the deviation during an interval of T_s, and the other is to estimate the total deviation for the whole duration. Considering the effectiveness, the average deviation is one of the quantitative methods to determine the dispersion for the database. Generally, average deviation indicates the maximum scale of scatter, and the lower average deviation represents less information lost owing to that the samples are approximately gathered under different intervals.

2) INFORMATION ENTROPY THEORY

Although the average deviation can represent the dispersion of the database under different sampling intervals, the results may fail to interpret the real content when the deviation is under varied distribution such as the parts of data surrounds the average while others contributes more for deviation. The employment of composition for the information is regarded as essential cogitation for improvement. More methods are necessary for describing the proportion of information distribution, and herein the information entropy is developed to evaluate the content of the discreated database [27].

The development of information entropy is an essential foundation for distribution of determined region, and the probability of each partition can be defined as equation (21). Herein, the minimum and maximum of each region are determined from the fluctuating database, and the numbers of the regions are divided as artificial selection. Additionally, the amount of information I can be defined as equation (22). It is worthy to mention that the probability is generally less than one, thus the logarithm of the probability is negative which is hard to interpret the content of information entropy. And the negative sign in equation (22) is to compensate the logarithm, and I_i is practically positive.

$$P(x_i) = \frac{h_l}{h_u} \frac{N(x_i)}{\sum_{j=1}^{K} N(x)}$$ (21)

$$I_i = -\log P(x_i)$$ (22)

$$H(x) = -C \sum_{i=1}^{N} P(x_i) I_i$$ (23)

$$H(x) = -\sum_{i=1}^{N} P(x_i) I_i$$ (24)

$$\sum_{i=1}^{l-1} h_{l-1} \leq \chi < \sum_{i=1}^{l} h_l$$ (25)

where: h_l and h_u are the lower/upper bound of the region; P is the probability of state x; $H(x)$ is the information entropy; C is the constant number; χ is the desecrated data.

Generally, the entropy of information is defined as equation (23), where $H(x)$ is associated with the distribution of data. To explore more effective information, the definition of information entropy composites expectation of information contents, and the utilization of logarithm guarantee the monotonic for method. Considering that the constant C has no contribution for the information entropy, the normalized entropy is adopted as equation (24). The monotonic information entropy indicates the larger entropy usually refers to effective content. Unfortunately, the direct estimation for probability of the equation leads to massive computation cost, and a method for substituting the probability with frequency is adopted to simplify the calculation, presented as equation (25). And the summarization of information entropy theory can be presented as follows:

Step 1: Initialization

Select the serial database, and calculate the length L of database and determine the upbound and lower bound.

Step 2: Division

Determine the number of categories n for division, and equally divide the length L into n parts. Classify the database into several departments.

Step 3: Calculation

Calculate the frequency of each departments, and substitute the probability with frequency. Estimate the information entropy.

III. EXPERIMENTS AND SIMULATION SCHEMES

In this section, the experimental batteries and testing facilities are presented, and the detailed simulation schemes are demonstrated for achieve comprehensive evaluation. Considering the operational applications, diverse stable/dynamic experiments are carried out to verify the precision and robustness of parameterization and SOC estimation under various intervals. Additionally, the average deviation and information entropy are developed to research the content of database. The general procedure of the manuscript is presented in Figure 3.

A. EXPERIMENTAL BATTERIES

A battery of N18650CL-29 is experimented to verify the comprehensive influence of sampling intervals. NCM 811 is developed as cathode material and has been widely promoted on electric vehicles because it can achieve high energy density. The related information of the tested battery are listed in TABLE 4. It is worthy to mention that the real capacity of the battery may not be consistent with nominal capacity, thus in this article, the real capacity based on capacity experiment is adopted as substitution. Considering the influence of temperature on batteries, all experiments are carried out in
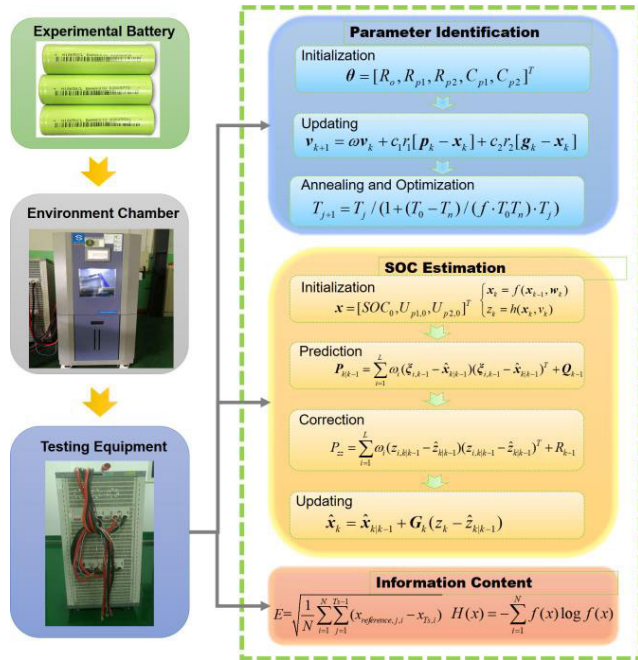
FIGURE 3. The general procedure of the manuscript.

TABLE 4. Characteristics of tested battery.

Item	Specification
Capacity	2600 mAh
Cathode material	NCM 811
Minimum voltage	2.5V
Maximum voltage	4.2V
Normal voltage	3.6V
Max discharging current	3C
Max charging current	1C
Energy density	225 Wh/kg

TABLE 5. List of testing equipment.

Item	Equipment Type
Charging/discharging tester	Neware CT-4004-5V30A-NA battery cycler
Environment chamber	Soyater ETE-GDW-150L environmental chamber
Monitor computer	Ryzen 5 3500U
Simulation tool	MATLAB

environment chamber and the testing equipment are listed in TABLE 5.

B. TESTING CONDITIONS

Considering the operational application, two categories of testing conditions are utilized to determine the stable/dynamic characteristics. Additionally, the pulse discharging experiment is carried out and the results are used for parameterization. The batteries are fully charged and then gradually discharge 10% of capacity with 1C current until the battery fully discharged. 1 hour for resting is performed between each discharging period. Additionally, the open circuit voltage can be identified as the voltage for each end of resting period. The availability of an accurate model will be ensured for BMS during the whole service lifespan. The other constant-current discharging and dynamic discharging

are to verify the parameter identification and SOC estimation. New European Driving Cycle (NEDC) and dynamic stress test (DST) are taken to verify the dynamic characteristics of both the identified parameters and SOC estimation [27]. The adopted operational conditions can be illustrated as Figure 4. It is worthy to mention that the batteries are tested in the environment chamber, and the temperature is set as 25 °C. The heat generation is neglected and the temperature of battery is assumed to be constant.
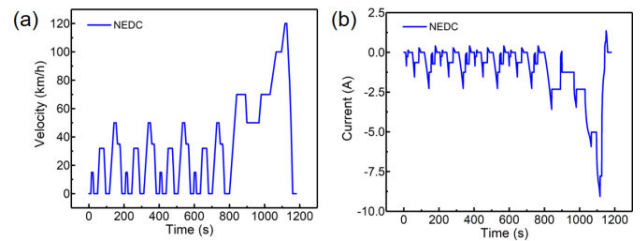

FIGURE 4. Current-time curves of the applied NEDC conditions. (a) the profile of velocity-time; (b) the transformed profile of current-time.

C. TEST SCHEMES

Various performances are essential to be verified for investigating the influences of sampling intervals. Thus, the serial simulation schemes are carried out, including precision and robustness analysis of parameterization and SOC estimation under different intervals. Herein, the sampling intervals are selected as 1 s, 2 s, 5 s, 6 s, 10 s, 15 s, 20 s, 30 s. The selection of sampling intervals is considering the current legislated institution or the applicational cloud-database for enterprises. Additionally, the average deviation and information entropy theory are developed to verify the content of discrete database. Considering the diverse impacts, the comprehensive schemes of testing are listed in TABLE 6. The results contribute to evaluate the comprehensive performance of sampling interval, and might deliver the optimum intervals for future design of cloud-database.

IV. RESULTS AND DISCUSSION

A. THE PRECISION ANALYSIS ON INTERVALS

Considering the discrepancy on stable and dynamic conditions, two categories of operational conditions are experimental as scheme 1-16. Herein, the 1C discharging is recognized as stable test, and the NEDC condition is adopted to activate the dynamic performances. The general results are presented in TABLE 6, and the analysis is demonstrated as follows.

A comparison of both parametrization and SOC estimation is carried out as Figure 5 to verify the precision on different sampling intervals. Three intervals, including 1 s, 6 s, 30 s, are simulated, and the reference is measured from the testing equipment. A maximum absolute error of 40 mV can be observed for the intervals less than 6 s, while the error is comparatively larger for other intervals. Similarly, the SOC estimation still presents a maximum absolute error of 4%, which is still satisfying the requirement of BMS.

TABLE 6. Testing schemes.

Item	Categories	Discharge Condition	Sampling interval/s	SOC initialization/%	Maximum absolute deviation of parameterization	Maximum absolute deviation of SOC estimation
1		1C	1	100	32.55	2.55%
2		1C	2	100	34.06	3.24%
3		1C	5	100	38.68	3.42%
4	Stable condition	1C	6	100	39.98	3.51%
5		1C	10	100	41.88	4.69%
6		1C	15	100	43.01	4.95%
7		1C	20	100	44.24	5.33%
8		1C	30	100	49.18	5.80%
9		NEDC	1	100	41.26	4.47
10		NEDC	2	100	45.39	4.43
11		NEDC	5	100	46.57	5.3
12	Dynamic condition	NEDC	6	100	46.46	5.42
13		NEDC	10	100	56.94	6.08
14		NEDC	15	100	75.3	6.73
15		NEDC	20	100	86.54	7.32
16		NEDC	30	100	90.59	8.27

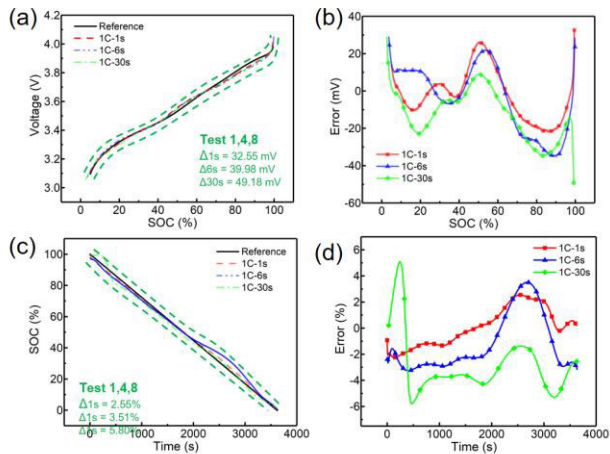| Item	Categories	Condition	Sampling interval/s	SOC initialization/%	Time for convergence
17		NEDC	1	80	159
18		NEDC	2	80	180
19		NEDC	5	80	200
20	Robustness analysis	NEDC	6	80	218
21		NEDC	10	80	230
22		NEDC	15	80	315
23		NEDC	20	80	500
24		NEDC	30	80	660

FIGURE 5. Comparisons for different sampling intervals. (a) and (b) comparison of parameterization; (c) and (d) comparison of SOC estimation based on 1C discharging.

FIGURE 6. Comparisons of different sampling intervals on parameter identifications. (a) 1s; (b) 2s; (c) 5s; (d) 6s; (e) 10s; (f) 15(s); (g) 20s; (h) 30s.

Additionally, the comparison of performances on NEDC for diverse sampling intervals are presented as Figure 6 and Figure 7. Generally, the maximum absolute error of 50 mV for parameter identification and approximate error of 6% for SOC can be achieved for intervals under 10 s on fluctuating dynamic conditions, while the larger ones usually lead to worse results.

The potential explanation of the increasing error might be that the larger sampling intervals enlarge the failure of ECMs, indicating that the long-term dynamic performances could
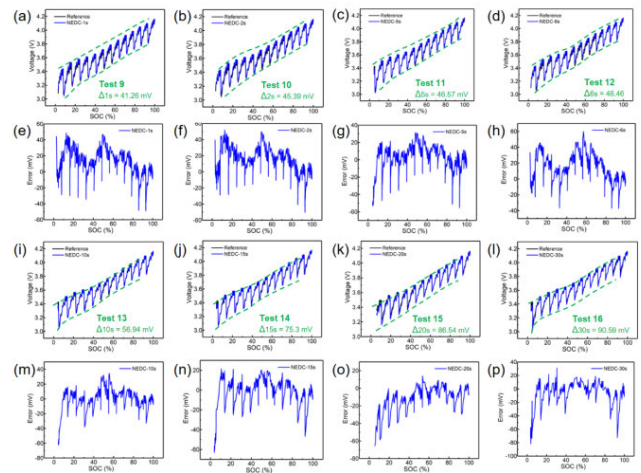
not be simulated by ECMs. Moreover, the raising information loss as the increasing of sampling intervals still could be attributed for the results. Considering the comprehensive performances on precision analysis, the sampling intervals between 1 s and 10 s might be preferable when to design the cloud-database for precision state estimation.

Additionally, similar phenomenon can be observed in parameter identification process. Illustrated as Table 6, both stable and dynamic conditions are performed for parameter identification by second-order equivalent model.
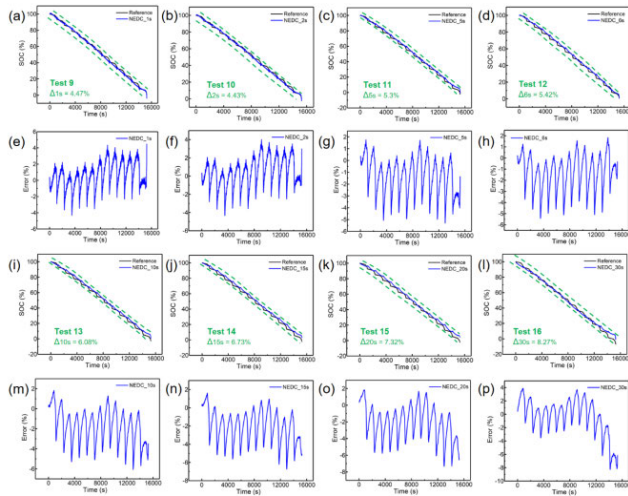
FIGURE 7. Comparisons of different sampling intervals on parameter identifications. (a) 1 s; (b) 2 s; (c) 5 s; (d) 6 s; (e) 10 s; (f) 15 s; (g) 20 s; (h) 30 s.

The maximum deviation of terminal voltage compared with experimental results indicates that less error can be obtained with more samplings, and a preferred period of sampling interval is considered to be 1-10 s.

B. THE ROBUSTNESS ANALYSIS ON INTERVALS

Considering the operation for cloud-controlling, the robustness for initialization deviation and interfered measurements is of crucial for improving the applicational performances. Herein, a simulation analysis for robustness based on initialization deviation under various sampling intervals is carried out, and the general results are presented as TABLE 6. A comparison is demonstrated in Figure 8, where the deviation is the same set as 20% and the intervals are selected as 1 s, 6 s, 10 s, 30 s.

The results demonstrate that the convergence time is increasing as the enlarging intervals, while the tendency is nonlinearly developed. Considering the general appropriate expectation of 240 s (4 min), the performance of intervals between 1s and 6 s presents the satisfactory speed for convergence. Thus, the recommended intervals for designing the cloud-controlling platform is between 1 s and 6 s. Additionally, the performance of robustness is associated with the covariance of the algorithm, and the artificial covariance might improve the results under other intervals.

Furthermore, considering the interferences on sensor, the fluctuating sampling may suffer from the deviation such as current and voltage and leads to error for SOC estimation. Herein, a simulated analysis is carried out as presented in Figure 9, where a random deviation on current under 10% capacity is applied to the sampled data. The results indicate that the SOC estimation under both few or large intervals has the ability for anti-interference compared with Coulomb counting (CC), which might be attributed to the closed-loop observer.
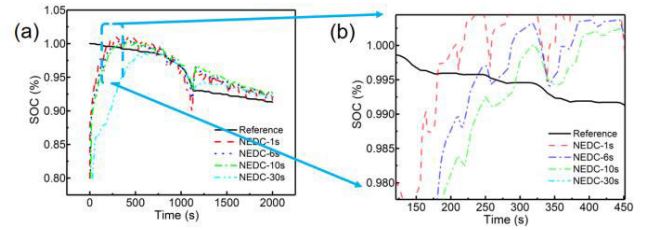

FIGURE 8. The comparisons on characteristics for correcting the initialization. (a) Convergence under 20% deviation; (b) the enlarged image.
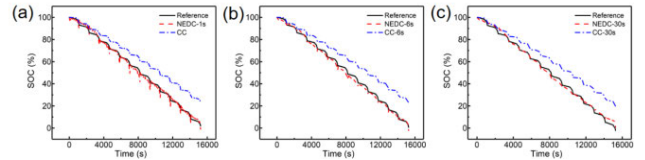

FIGURE 9. The comparisons on ability for anti-interference under variable sampling intervals. (a) 1 s; (b) 6 s; (c) 30 s.

TABLE 7. Results of average deviation analysis.

Sampling interval	Average Deviation			
	1C-Current	1C-Voltage	NEDC-Current	NEDC-Voltage
2	7.09E-04	9.09E-04	0.1329	0.0056
5	0.0015	0.0047	0.4755	0.0211
6	0.0017	0.0063	0.5346	0.024
10	0.0024	0.0141	0.9168	0.0433
15	0.003	0.0253	1.5786	0.0742
20	0.0038	0.0383	2.1783	0.1044
30	0.0051	0.0687	3.2297	0.1621

C. THE CONTENT ANALYSIS ON INTERVALS

The average deviation and information entropy theory are utilized for evaluating the essential contents of the discrete database, and the results are presented as TABLE 7 and TABLE 8. Considering the definition of information entropy theory, the larger entropy generally indicates a comprehensive content compared with the originated database. Herein, the comparison between 1C discharging and NEDC is carried out, and the results are demonstrated in Figure 10.

TABLE 8. Results of average information entropy.

Sampling interval	Information Entropy	
	1C discharge	NEDC
2	121.7221	157.2728
5	105.0873	160.0506
6	109.5328	156.9554
10	95.8103	160.581
15	93.57	158.4636
20	86.1847	161.0328
30	83.5879	151.8247

The average deviations for both conditions present an approximate linear increase with intervals. However, the general deviation of 1C discharging is larger than that under NEDC condition. The potential reason might be that the fluctuating samplings compensate the information loss, while that might be failed under stable conditions as the polarization is rather stable.
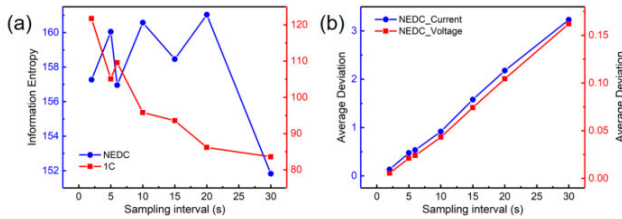
FIGURE 10. The analysis of information content of the desecrated database under stable/dynamic conditions. (a) information entropy; (b) average deviation.

The information entropy presents distinct results for two conditions. The entropy is approximate linear decrease as the increasing of intervals for stable condition. The results could be attributed to stable polarization where the voltage is on ordinary distribution, but the larger sampling intervals lead to the massive information loss. However, the fluctuating database for NEDC condition contributes to the compensation of data loss. The potential interpretation might be that the dynamic performance is time-varying but the samplings are generally surrounding the average as the fluctuating current applied on the battery.

The analysis of the content indicates that the information lost is associated with the operational condition and the degree of fluctuation. Based on the experimental results, the larger sampling intervals might be applied for dynamic discharging of electric vehicles, while a smaller interval would be appreciated for charging process. These results obtained can be instructional on the designs of intelligent battery management systems and their further interactional control based on the cloud-platform.

V. DISCUSSION

A comprehensive comparison of the performances on diverse sampling intervals is presented as TABLE 9. The decreasing

TABLE 9. Evaluation of the comprehensive performances under diverse intervals.

Sampling interval /s	Precision on parameterization	Precision on SOC estimation	Robustness	Information content under stable condition	Information content under dynamic condition
1	☆☆☆☆☆	☆☆☆☆☆	☆☆☆☆☆	☆☆☆☆☆	☆☆☆
2	☆☆☆☆	☆☆☆☆☆	☆☆☆☆	☆☆☆☆	☆☆
5	☆☆☆	☆☆☆☆	☆☆☆☆	☆☆☆	☆☆☆
6	☆☆☆	☆☆☆☆	☆☆☆	☆☆☆	☆☆☆☆
10	☆☆	☆☆☆	☆☆☆	☆☆	☆☆☆☆☆
15	☆☆	☆☆	☆☆	☆☆	☆☆☆☆
20	☆	☆	☆	☆	☆☆☆
30	☆	☆	☆	☆	☆

precision of parameterization and SOC estimation might be attributed that the dynamic battery model fails to simulate the fluctuating data under large sampling intervals, and the improvements on modelling such as the meticulous electrochemical model could be effective ones. The robustness is associated with the iteration times, while the larger intervals lead to a higher period for convergence. Considering the applicational operation, it might be preferable for initialization under less intervals to obtain the better convergence speed. As for information content, the results exhibit opposite appearance for stable/dynamic conditions. Premeditating the storage cost and the information entropy, it might be appropriate for few intervals under stable condition such as fast charging, and large intervals for dynamic discharging conditions.
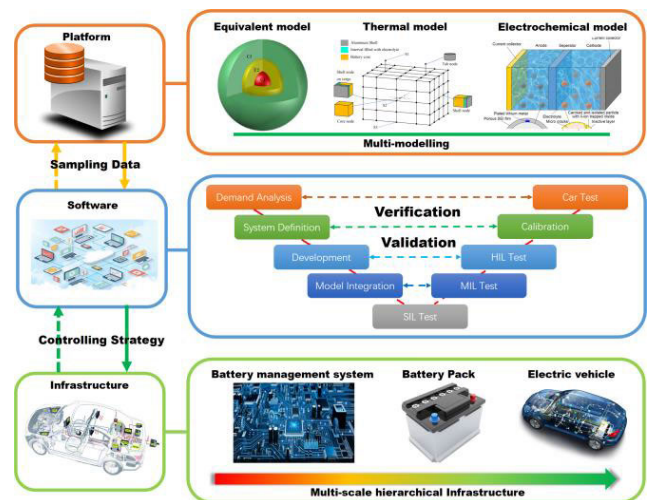

FIGURE 11. The possible hierarchical framework of EV power batteries based on cloud-controlling.

The possible hierarchical framework of EV power batteries based on cloud-controlling is presented in Figure 11. The framework includes the basic infrastructure of power battery system, software and cloud control platform. The cloud control platform mainly consists of data storage and battery state estimations, including the data-driven and model driven battery state estimations (mainly SOC, state of energy (SOE), state of power (SOP), state of health (SOH), state of safety (SOS)), energy management and power system pre-warning. The interacting software group contribute to the reliance of the system, and the collected information from infrastructures are uploaded to the cloud-platform, where the sampling interval crucially matters to prediction and accuracy. The basic infrastructure is associated with fundamental direct control for vehicles, and the achievements of cloud controlling platform is dependent on the reliable infrastructure. The main concept of the hierarchical processing framework is to sampling the information from basic infrastructure and then uploading to the flatform by both hardware and software. The controlling strategy can be developed and optimized upon sufficient data and model processing applying cloud-

platform, and the associated functions can be achieved with precise algorithms, which ensures accurate real-time prediction and interactional management for full lifespan management of EV power battery systems. As one of essential factors for influencing the effectiveness of database, the sampling intervals determine the proportion of essential information and other dynamic kinematic characteristics. Considering the operational application for hierarchical processing framework, the selection of the sampling intervals should be fundamental on the purpose for cloud-database design.

More issues associated with the variable sampling intervals could be taken into consideration for future research. For example, the theory on electrochemical model which analyzes the internal reactions on degradation remains a challenge, and the influences on sampling intervals are still questionable for model construction. Additionally, the phenomenon of data-loss is still out of consideration, which might result in the cumulative error for iterative estimation. As one of the normal operations, vehicles might drive pass the skyscrapers or tunnels where the vehicles could stop the communication with cloud-platforms, possibly causing a loss of information. Compared with serial data-packs. Further research is still necessary to adjudicate between the sampling intervals and BMS.

VI. CONCLUSION

In this article, a comprehensive research on sampling intervals is carried out for delivering the according guidance for future cloud-database/controlling design. Diverse precision and robustness investigations under various intervals are presented and the content is verified based on information entropy theory. Herein, a method of particle swarm optimization - simulated annealing is carried out for parameterizing the battery model, and to the state-of-art, the 5th-order spherical simplex-radial cubature Kalman filter is developed for SOC estimation. The implementation of second-order equivalent circuit model is exhibited and a battery of NCM 811 cathode is experimental for validation. The precision, robustness and content analysis are carried out to guide the potential system design based on future cloud-controlling platform.

The article highlights the diverse analysis of comprehensive performance for BMS under different sampling intervals, and the abundant simulation enhances the validation of the results. Considering the objective of constructing the cloud-database, the potential sampling intervals are separately delivered to enhance the performances. Based on the PSO-SA and 5th-SSRCKF methods, the precision of discrete state estimation is discussed, and an interval between 1s and 10s is suggested to satisfying the demand of BMS. Considering the applicational operation, an interval between 1s and 5s is recommended fundamental on robustness analysis. Additionally, the results of information content indicate that the sampling interval could be adaptive as the changing of driving pattern, which might contribute to the design of cloud-controlling.

The results confirm the potential application of cloud-controlling and more functions can be extended based on the proposed framework. The developed algorithm and conclusion contribute to various functions, mainly including data parameterization, battery state estimations, energy management and power system pre-warning, guiding the future design of the battery management system upon cloud-controlling platform in the broad framework of **CHAIN**.

REFERENCES

[1] Z. Li, J. Huang, B. Y. Liaw, and J. Zhang, "On state-of-charge determination for lithium-ion batteries," *J. Power Sources*, vol. 348, pp. 281–301, Apr. 2017.

[2] S. Wang, D.-I. Stroe, C. Fernandez, C. Yu, C. Zou, and X. Li, "A novel energy management strategy for the ternary lithium batteries based on the dynamic equivalent circuit modeling and differential Kalman filtering under time-varying conditions," *J. Power Sources*, vol. 450, Feb. 2020, Art. no. 227652.

[3] S. Khaleghi, Y. Firouz, J. Van Mierlo, and P. Van den Bossche, "Developing a real-time data-driven battery health diagnosis method, using time and frequency domain condition indicators," *Appl. Energy*, vol. 255, Dec. 2019, Art. no. 113813.

[4] Y. Li, K. Liu, A. M. Foley, A. Zälke, M. Berecibar, E. Nanini-Maury, J. Van Mierlo, and H. E. Hoster, "Data-driven health estimation and lifetime prediction of lithium-ion batteries: A review," *Renew. Sustain. Energy Rev.*, vol. 113, Oct. 2019, Art. no. 109254.

[5] S. Yang, R. He, Z. Zhang, Y. Cao, X. Gao, and X. Liu, "CHAIN: Cyber hierarchy and interactional network enabling digital solution for battery full-lifespan management," *Matter*, vol. 3, no. 1, pp. 27–41, Jul. 2020, doi: 10.1016/j.matt.2020.04.015.

[6] X. Feng, "A reliable approach of differentiating discrete sampled-data for battery diagnosis," *Transportation*, vol. 3, Feb. 2020, Art. no. 100051.

[7] Y. Li, M. Vilathgamuwa, T. Farrell, S. S. Choi, N. T. Tran, and J. Teague, "A physics-based distributed-parameter equivalent circuit model for lithium-ion batteries," *Electrochimica Acta*, vol. 299, pp. 451–469, Mar. 2019.

[8] C. Yang, X. Wang, Q. Fang, H. Dai, Y. Cao, and X. Wei, "An online SOC and capacity estimation method for aged lithium-ion battery pack considering cell inconsistency," *J. Energy Storage*, vol. 29, Jun. 2020, Art. no. 101250.

[9] S.-L. Wang, C. Fernandez, W. Cao, C.-Y. Zou, C.-M. Yu, and X.-X. Li, "An adaptive working state iterative calculation method of the power battery by using the improved Kalman filtering algorithm and considering the relaxation effect," *J. Power Sources*, vol. 428, pp. 67–75, Jul. 2019.

[10] W. Yan, B. Zhang, W. Dou, D. Liu, and Y. Peng, "Low-cost adaptive lebesgue sampling particle filtering approach for real-time li-ion battery diagnosis and prognosis," *IEEE Trans. Autom. Sci. Eng.*, vol. 14, no. 4, pp. 1601–1611, Oct. 2017.

[11] J. Hong, Z. Wang, W. Chen, L.-Y. Wang, and C. Qu, "Online joint-prediction of multi-forward-step battery SOC using LSTM neural networks and multiple linear regression for real-world electric vehicles," *J. Energy Storage*, vol. 30, Aug. 2020, Art. no. 101459.

[12] W. Zhang, L. Wang, L. Wang, and C. Liao, "An improved adaptive estimator for state-of-charge estimation of lithium-ion batteries," *J. Power Sources*, vol. 402, pp. 422–433, Oct. 2018.

[13] F. Yang, Y. Xing, D. Wang, and K.-L. Tsui, "A comparative study of three model-based algorithms for estimating state-of-charge of lithium-ion batteries under a new combined dynamic loading profile," *Appl. Energy*, vol. 164, pp. 387–399, Feb. 2016.

[14] D. Li, J. Ouyang, H. Li, and J. Wan, "State of charge estimation for LiMn2O4 power battery based on strong tracking sigma point Kalman filter," *J. Power Sources*, vol. 279, pp. 439–449, Apr. 2015.

[15] Y. Wang, C. Zhang, and Z. Chen, "A method for state-of-charge estimation of LiFePO4 batteries at dynamic currents and temperatures using particle filter," *J. Power Sources*, vol. 279, pp. 306–311, 2015-01-01 2015.

[16] J. Yang, Y. Cai, C. Pan, and C. Mi, "A novel resistor-inductor network-based equivalent circuit model of lithium-ion batteries under constant-voltage charging condition," *Appl. Energy*, vol. 254, Nov. 2019, Art. no. 113726.

[17] H. Pang, L. Mou, L. Guo, and F. Zhang, "Parameter identification and systematic validation of an enhanced single-particle model with aging degradation physics for li-ion batteries," *Electrochimica Acta*, vol. 307, pp. 474–487, Jun. 2019.

[18] Q.-K. Wang, Y.-J. He, J.-N. Shen, Z.-F. Ma, and G.-B. Zhong, "A unified modeling framework for lithium-ion batteries: An artificial neural network based thermal coupled equivalent circuit model approach," *Energy*, vol. 138, pp. 118–132, Nov. 2017.

[19] K. Saleem, K. Mehran, and Z. Ali, "Online reduced complexity parameter estimation technique for equivalent circuit model of lithium-ion battery," *Electr. Power Syst. Res.*, vol. 185, Aug. 2020, Art. no. 106356.

[20] P. Vyroubal and T. Kazda, "Equivalent circuit model parameters extraction for lithium ion batteries using electrochemical impedance spectroscopy," *J. Energy Storage*, vol. 15, pp. 23–31, Feb. 2018.

[21] X. Song, Y. Lu, F. Wang, X. Zhao, and H. Chen, "A coupled electro-chemo-mechanical model for all-solid-state thin film li-ion batteries: The effects of bending on battery performances," *J. Power Sources*, vol. 452, Mar. 2020, Art. no. 227803.

[22] M. Kim, H. Chun, J. Kim, K. Kim, J. Yu, T. Kim, and S. Han, "Data-efficient parameter identification of electrochemical lithium-ion battery model using deep Bayesian harmony search," *Appl. Energy*, vol. 254, Nov. 2019, Art. no. 113644.

[23] X. Lai, S. Wang, S. Ma, J. Xie, and Y. Zheng, "Parameter sensitivity analysis and simplification of equivalent circuit model for the state of charge of lithium-ion batteries," *Electrochimica Acta*, vol. 330, Jan. 2020, Art. no. 135239.

[24] I. Esfandiarpour-Boroujeni, E. Karimi, H. Shirani, M. Esmaeilizadeh, and Z. Mosleh, "Yield prediction of apricot using a hybrid particle swarm optimization-imperialist competitive algorithm- support vector regression (PSO-ICA-SVR) method," *Scientia Horticulturae*, vol. 257, Nov. 2019, Art. no. 108756.

[25] F. Javidrad, M. Nazari, and H. R. Javidrad, "Optimum stacking sequence design of laminates using a hybrid PSO-SA method," *Compos. Struct.*, vol. 185, pp. 607–618, Feb. 2018.

[26] J. Behnamian and S. M. T. Fatemi Ghomi, "Development of a PSO–SA hybrid Metaheuristic for a new comprehensive regression model to time-series forecasting," *Expert Syst. Appl.*, vol. 37, no. 2, pp. 974–984, Mar. 2010.

[27] C. Savari, R. Sotudeh-Gharebagh, G. Kulah, M. Koksal, and N. Mostoufi, "Detecting stability of conical spouted beds based on information entropy theory," *Powder Technol.*, vol. 343, pp. 185–193, Feb. 2019.

[28] F. Sun, X. Meng, C. Lin, and Z. Wang, "Dynamic stress test profile of power battery for electric vehicle," *Trans. Beijing Inst. Technol.*, vol. 30, no. 3, pp. 297–301, 2010.

YAOGUANG CAO received the B.S. degree in thermal energy and power engineering from Beihang University, in 2010, and the M.S. degree in automotive engineering, in 2012. He is currently pursuing the Ph.D. degree in automotive engineering with Beihang University.

He had a work experience serving in the EV Project Management Office of High Technology Research and Development Center, Ministry of Science and Technology of China, from 2013 to 2015. His research interests include intelligent decision and planning strategy for autonomous vehicles, automotive cybersecurity, and intelligent ADAS sensors. His awards and honors include the First Prize of Technical Invention by China Automatic S&T and the Second Prize of Sci-Tech Progress by the Ministry of Education.

SIDA ZHOU is currently pursuing the master's degree in automotive engineering with Beihang University. From 2018 to 2020, he had major research concentrate on the battery management for electric vehicles. His research interests include intelligent battery management systems, battery state estimation, equalization technology of serial battery pack, and thermal management systems.

YANG HUA received the B.S. degree in electrical engineering from Tsinghua University, Beijing, China, in 2000, and the M.S. degree in electrical engineering from the Institute of Electrical Engineering, Chinese Academy of Sciences, Beijing, in 2003. He is currently pursuing the Ph.D. degree in new energy vehicle engineering with Beihang University, Beijing.

His research interests include battery management, electric vehicle control, motor control, and vehicle electronics.

XINAN ZHOU is currently pursuing the master's degree in new energy vehicle engineering with Beijing University, China. From 2018 to 2020, he had major research concentrate on the modeling of lithium ion battery for electric vehicles and software development for battery management system. His research interests include battery aging mechanism, fast charging strategy, and battery modeling on electrochemical-thermal models.

SHICHUN YANG (Member, IEEE) is currently the Dean of the School of Transportation Science and Engineering, Beihang University, leading personnel of Scientific and Technological Innovation in the National Ten-Thousand Talents Program, leading personnel among the young and middle-aged in the Ministry of Science and Technology, National Outstanding Scientific and Technological Worker. He is also the Vice Chairman of the Electric Vehicle Division, National Technical Committee of Automobile Standardization (NTCAS), an Expert of Road Vehicle Specialized Committee of China Intelligent Transportation System Association (CTTSA), and the Vice Chairman of SAE Vehicle Safety and Information Security Technical Committee. His research mainly works on scientific and technological research for EV power system safety, high-efficient optimal theory, and integrated control. He received the National Second Prize for Progress in Science and Technology, the First Prize of Technical Invention and Sci-Tech Progress by China Automatic S&T, the Second Prize of Sci-Tech Progress, and the Technical Invention by the Ministry of Education.

XINHUA LIU is currently an Assistant Professor at the School of Transportation Science and Engineering, Beihang University, a Visiting Lecture at the Dyson School of Design Engineering, Imperial College London, U.K., and a Lab Manager of the New Energy Vehicle Institute, Beihang University (Zhejiang). She has published more than 54 articles, including in *Matter*, *Advanced Materials*, *Energy Storage Materials*, and *Advanced Science*. Her research interests include the interface between electrochemical science and engineering applying a digital process, including designer energy materials for various energy storages, model-driven microstructure optimization for high performance batteries, cloud control-based battery degradation mechanism, diagnose, and battery management system design.

● ● ●